WATER-COOLED FAST-RESPONSE WALL-STATIC PRESSURE PROBES FOR HARSH COMBUSTOR ENVIRONMENT APPLICATIONS

Julien Clinckemaillie
Turbomachinery and Propulsion Department
von Kármán Institute for Fluid Dynamics

Fabrizio Fontaneto
Turbomachinery and Propulsion Department
von Kármán Institute for Fluid Dynamics

Jean-Louis Champion-Réaud
Safran Tech

Éric Bouty
Safran Helicopter Engines

Carlos Mendes
Safran Tech

ABSTRACT

The present paper discusses the design methodology for a water-cooled fast-response wall-static pressure probe intended for measurements in the combustion chamber of gas turbines, as well as the results from a series of tests performed with the prototype of the probe mounted in the primary zone of the combustion chamber of a turboshaft engine test rig. The first part of the present paper reviews the design methodology of a water-cooled fast-response wall static pressure probe intended for measurements of combustion noise and instabilities in gas turbine combustors, describing the optimization of measurement performance in terms of frequency bandwidth ([0 – 40kHz]) as well as the design of the cooling layout ensuring the sensor's integrity within a harsh environment. The second part of the paper focuses on the analysis of the results obtained from trial tests performed using the probe prototype mounted in the primary zone of the combustion chamber of a helicopter engine test rig. The strengths and strong potential for further growth of the current probe design are highlighted, while its shortcomings and (short-term) solutions to these shortcomings are also discussed.

NOMENCLATURE

Roman Symbols

f	Frequency
P	Pressure
PS	Power Spectrum
RTV	Room temperature vulcanizing
SiC	Silicon-carbide
SOI	Silicon-on-Insulator
SPL	Sound Pressure Level (Ref. pressure $P_{ref} = 2 \times 10^{-5}$ Pa)
T	Temperature
TF	Transfer function
V	Voltage

Greek Symbols

β	Kurtosis
γ	Skewness
σ	Standard deviation

Subscripts

avg	Averaged
gas	Gas path
n	Natural
P	Pressure
S	Sense temperature
zero-flow	Zero-flow conditions

INTRODUCTION

In an effort to extend the knowledge around combustion noise and combustion instabilities while supporting the development of more performant combustion control systems, the availability of fast-response pressure measurement devices able to operate in the harsh environment of gas turbine combustors is fundamental and remains a significant challenge. The severe heat load at which they are submitted forces the adoption of an efficient cooling layout to keep the continuously immersed probe material well below its maximum operating temperature.

This constraint becomes even more critical when the fragile sensing element of conventional off-the-shelf piezo-resistive fast-response pressure transducers is considered. Their large bandwidth (150 kHz – 1 MHz) over a wide pressure range (0.35 – 70 bar), as well as their ability to measure both the steady and (periodic or random) unsteady component of pressure makes them the most widely used type of sensors for fast-response static or total pressure measurements. The datasheets of conventional off-the-shelf miniature piezo-resistive pressure transducers quote a maximum operating temperature range up to 273 °C, while state-of-the-art SOI (silicon-on-insulator) [1] and SiC (silicon-carbide) [2] sensors allow the use of fast-response pressure sensors at temperatures up to 505 °C and 605 °C respectively. However, in order to reach even higher temperatures in a continuously immersed configuration, efficient sensor cooling becomes obligatory for their protection.

1

Ferguson and Ivey have demonstrated the effectiveness of water-cooled and air-cooled piezo-resistive sensors for the measurement of unsteady wall-static pressure in a hot environment. They reported safe operation up to 800 °C for the air-cooled and water-cooled configuration [3], however in their study, they pointed out the significant benefit of using water as the cooling medium owing to its much higher specific heat capacity. One of their most recent studies on the concept of air-cooling jackets around commercial piezo-resistive high-bandwidth pressure transducers has demonstrated a safe temperature capability up to 900 °C [4]. One of the aims of the presented work is to further push the envelope in terms of temperature capability for unsteady pressure measurements.

In the framework of the EU FP6 project HEATTOP, Brouckaert et al. and Mersinligil et al. designed a fast-response total pressure probe using a single SOI piezo-resistive sensor water-cooled by means of a high-pressure cooling system [5, 6]. The sensor was able to survive an intermediate-pressure combustion rig measurement campaign where it was fully immersed into the hot gas stream of the flame tube characterized by a bulk temperature of 1730 °C. Under the most severe conditions, the fragile sensing element membrane temperature was kept below 205 °C, with a coolant flow rate of 10 l/min at 32 bar water pressure. Owing to its demonstrated effectiveness, the cooling layout adopted for this water-cooled fast-response total pressure probe serves as the main basis for the probe cooling layout design utilized in the present paper.

PROBE DESIGN

In order to measure complex combustion instabilities and acoustic phenomena taking place in the combustor of gas turbines, the following design specifications are required:

- Measurement of both the steady and (periodic and random) unsteady components of the liner wall-static pressure
- A usable frequency bandwidth up to at least 40 kHz, with a flat response of ± 1 dB in the $[0 - 5]$ kHz frequency range of interest
- A highly robust and reliable probe design able to withstand the harsh conditions of the combustion chamber environment (FIGURE 2) characterized by gas temperatures up to $T_{gas} = 1650$ °C and pressure levels up to $P = 15$ bar
- An as-small-as-possible probe head size for adequate spatial resolution and minimal intrusiveness

These design requirements led to the adoption of an off-the-shelf ultra-miniature high-temperature piezo-resistive XCE-062 250PSIA Kulite sensor as pressure sensing element of choice. Its small

dimensions (1.7 mm in diameter), high signal-to-noise ratio, relative ease of use and adequate operating temperature range (from -55 to 273 °C) all favor its adoption for the proposed probe design.

FREQUENCY BANDWIDTH

In order to achieve the desired frequency bandwidth of 40 kHz, the sensor is mounted in a cavity slightly recessed from the probe tip (FIGURE 1). This small recess, combined with a protective screen, is used to safeguard the sensing element's integrity: the recessed layout offers protection from significant convective heat fluxes as the cavity is characterized by quasi-stagnant flow, while the perforated screen shields the sensor from direct line-of-sight with hot liner walls and radiant flames. Moreover, this layout offers a significant protection against direct particle impacts.
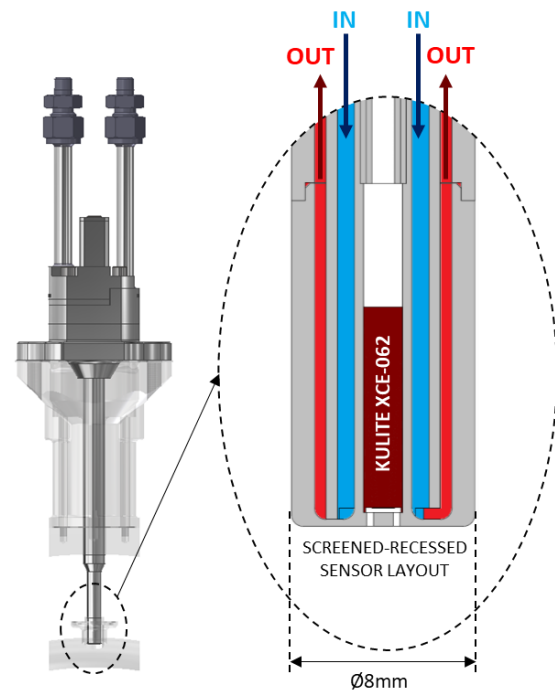

FIGURE 1: PROBE DESIGN – COOLING LAYOUT AND SCREENED-RECESSED SENSOR LAYOUT

However, the main downside of such a screened-recessed layout is the deteriorated usable flat-response bandwidth of the sensor due to the introduction of a resonant mode at a frequency much lower than the resonant frequency of the sensor. Indeed, the line-cavity system that is effectively formed by the screened-recessed sensor layout will behave as a strongly damped second order system with a peak amplitude at a certain resonance frequency. The screen is constituted of 8 holes of Ø0.3 mm with a line length of 0.6 mm, and the cavity is characterized by a diameter of Ø1.5 mm and a length of 0.2 mm. Theoretical models, such as the Hougen and Helmholtz resonator models [7, 8], indicate a resonant frequency of the screened-

recessed layout between 42 kHz and 61 kHz (depending on the investigated model) at ambient temperature, slightly above the required frequency bandwidth of 40 kHz. Furthermore, it should be noted that the gas temperature in the recessed cavity is expected to be greater than ambient temperature, which will further extend the frequency bandwidth as the resonance frequency increases with increasing gas temperature [4, 5].

PROBE COOLING LAYOUT

One of the main objectives of the probe design is to cool the sensing element down to keep the sensor operating temperature at around 100 °C, thereby keeping temperature effects on the pressure measurement to a minimum. To this end, coolant feed and return channels are incorporated into the probe and around the fragile sensor area (FIGURE 1). Due to integration constraints, the probe head immersed in the HP bypass annulus and flush with the inner combustor liner wall (FIGURE 2) has an outer diameter fixed at Ø8 mm. From this constraint and from the constraint imposed by the outer diameter of the sensing element, the annular coolant feed channel width is set to 0.75 mm and the annular coolant return channel width is set to 0.5 mm. As the probe will be used in a controlled and ground-based gas turbine testing environment, distilled water is chosen as the coolant of choice thanks to its high specific heat capacity and its wide availability and ease of use. For the series of tests presented in this paper, the probe was cooled using an external cooling system consisting of a 50 l distilled water reservoir, a high-pressure pump able to deliver up to 2 l/min of coolant through the probe, and a dedicated R407C refrigerant-based heat exchanger rated at 7 kW of cooling capacity.
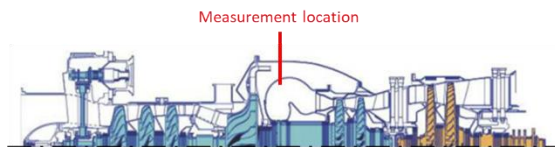
FIGURE 2: SAFRAN TECH BEARCAT TEST RIG [10] – SAFRAN HELICOPTER ENGINES MAKILA TURBOSHAFT GAS TURBINE

Based on a thorough evaluation of the overall heat transfer from the combustion chamber environment to the immersed probe, the effectiveness of the employed cooling layout has been assessed using a reduced-order correlation-based quasi-2D conjugate heat transfer model, as well as by means of 3D RANS conjugate heat transfer simulations. The survivability of the sensing element in the harsh combustion chamber environment has been demonstrated using both approaches, with probe surface temperatures remaining below 190 °C and sensor temperatures remaining below 135 °C for coolant flow rates ranging between 0.5 and 2.0 l/min. A thorough description of the methodology employed to design the internal cooling layout can be found in [9].

### PROBE PROTOTYPE ASSEMBLY AND CALIBRATION

After a thorough critical review of the probe design methodology, a first prototype of the probe has been manufactured and assembled. At several critical stages of the probe assembly, various minor checks have been performed: leakproofness of the probe cooling layout, evaluation of the adequacy of the cooling system's high-pressure pump with respect to the pressure losses through the cooling channels, and coherence of the output signals of the sensor. Once fully assembled, the probe prototype was evaluated in terms of sensor sensitivity (static calibration) and in terms of frequency bandwidth (dynamic calibration).

STATIC CALIBRATION

In order to not only retrieve pressure from the sensor, but also temperature (for the sake of evaluating the effectiveness of the probe sensor cooling), the Kulite sensor is used with an active compensation method, effectively yielding two output signals. The output signal V_P is primarily proportional to pressure, while the output signal V_S is a function of temperature. Hence, in order to achieve the static calibration of the sensor, a pressure calibration ranging from 0.6 to 3.4 bar (absolute) with intervals of 0.4 bar has been repeated for 5 temperature levels ranging between 20 °C and 120 °C with intervals of 25 °C, yielding a total of 45 calibration points. For each combination of pressure and temperature, the output signals V_P and V_S are acquired for 1 s at a sampling frequency of 100 kHz. The raw output signals V_P and V_S are time-averaged and the obtained calibration data are then fitted onto two separate polynomial surfaces (FIGURE 3) as expressed in Equations 1 and 2.

$$P = c_{P00} + c_{P10}V_P + c_{P11}V_PV_S + c_{P01}V_S + c_{P02}V_S^2 \qquad \text{Eq. (1)}$$

$$T = c_{T00} + c_{T10}V_P + c_{T11}V_PV_S + c_{T01}V_S + c_{T02}V_S^2 \qquad \text{Eq. (2)}$$
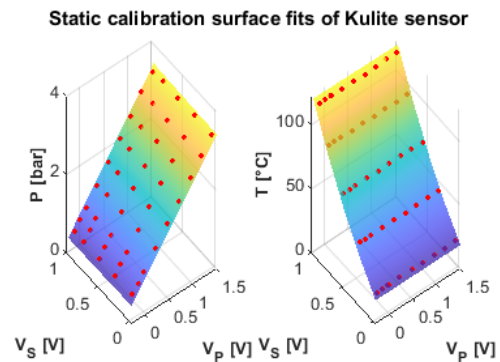
FIGURE 3: STATIC CALIBRATION OF KULITE SENSOR – PRESSURE (LEFT) AND TEMPERATURE (RIGHT) SURFACE FITS

DYNAMIC CALIBRATION

The dynamic response of the sensor is governed by the acoustic resonance of the line-cavity system formed by the screened-recessed sensor layout, theoretically evaluated between f_n = 42 kHz and f_n = 61 kHz depending on the model used. This purely theoretical approach has been further consolidated by performing shock-tube tests on the probe prototype, where the probe's dynamic response to an instantaneous pressure step is measured. On FIGURE 4, the experimentally obtained raw transfer function, averaged over 15 tests, is shown in grey, while a second-order transfer function model, fitted onto the experimental transfer function, is shown in red. From this series of experimental tests, the natural resonance frequency of the screened-recessed layout is experimentally measured to be f_n = 45 kHz, with a flat ±1 dB response up to 10 kHz, the wiggles at 4 – 5 kHz being caused by post-shock disturbances related to the shock-tube rig and not the screened-recessed layout.
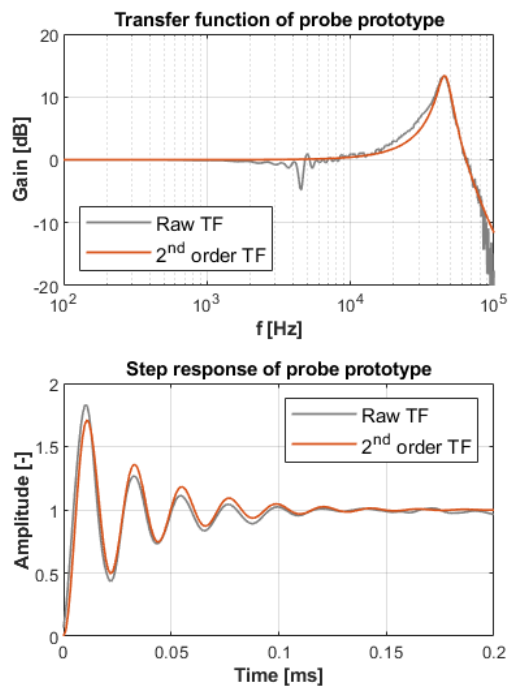
FIGURE 4: DYNAMIC CALIBRATION OF PROBE PROTOTYPE

MEASUREMENT CAMPAIGN

Following the static and dynamic calibration of the probe, the probe prototype was installed in the measurement plane corresponding to the primary zone of the combustion chamber flame tube of the Safran Tech Bearcat test rig [10], which is based on a Safran Helicopter Engines Makila turboshaft gas turbine (FIGURE 2). Before launching the test campaign, the following actions were performed:

- The flushness of the probe tip with respect to the inner liner wall of the combustor flame tube was checked by means of an endoscopic inspection
- The probe sensor was connected to the test rig conditioning and acquisition systems, and the output signals were verified
- The probe coolant feed and return lines were connected to the test rig cooling system, and the effective coolant flow rate through the probe was roughly estimated between 0.5 and 1.5 l/min, theoretically in line with a satisfactory sensor cooling

BACKGROUND NOISE

In order to evaluate the background noise of the probe sensor and its full measurement chain, 116 acquisitions of 5 seconds each were performed at a sampling frequency of 20 kHz under zero-flow conditions, i.e. with the Safran Helicopter Engines Makila turboshaft gas turbine of the Bearcat test rig not running. The statistical mean, standard deviation, skewness and kurtosis parameters of each measurement point are shown in FIGURE 5. As can clearly be observed, the mean value corresponds to the ambient pressure with a low standard deviation around the mean value ($P_{zero-flow}$ = [1.008 ± 0.005] bar). The skewness ($\gamma_{P,zero-flow} \approx 0$) and kurtosis ($\beta_{P,zero-flow} \approx 3$) values are consistent with a normal Gaussian distribution around the mean value. The same conclusion was derived from the temperature measurements (not shown), where the mean value corresponds to the ambient temperature with a low standard deviation around the mean value ($T_{zero-flow}$ = [15.5 ± 0.1] °C) and with skewness and kurtosis values once again in line with a normal Gaussian distribution.

The power spectrum of the background noise, expressed in dB_{SPL} and averaged over the 116 acquisitions, is shown in FIGURE 6. The expression of the background noise in terms of dB_{SPL} deserves a small but important comment: although this expression is typically used for acoustic sound pressure levels, the background noise in this case is entirely electronic in nature, as the background acoustic noise during the zero-flow acquisitions were well within the [40 – 60] dB_{SPL} range given the quiet laboratory environment in which the measurements were acquired, but was drowned by several orders of magnitude by the higher-powered inherent electronic noise injected by the sensor, the conditioner, and the acquisition system. Consequently, the sensor used with the prototype, namely the Kulite XCE-062 250 PSIA, can be considered as a microphone with a very high noise floor not suited for acoustic measurements of relatively quiet phenomenons. From 0 to 2 kHz, the background noise progressively decreases by 10 dB_{SPL}, while the 50 Hz cycles of the power grid,

along with its odd harmonics, are clearly observed. Beyond 2 kHz, the background noise remains constant, with local narrowband peaks around 2.7 kHz, 3.7 kHz and 4 kHz (supplemented by their even harmonics). The origin of these peaks has not been identified.
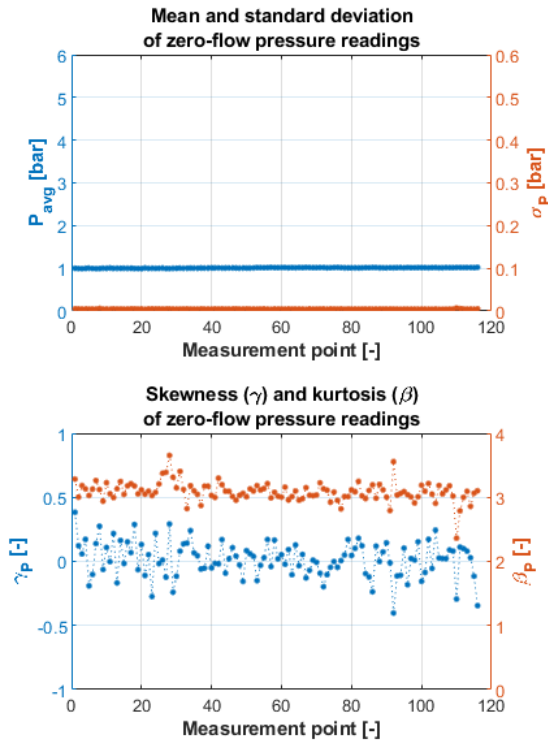

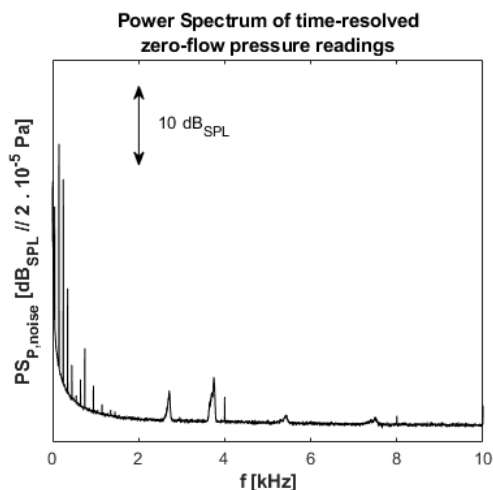**FIGURE 5:** STATISTICAL MOMENTS OF ALL 116 ZERO-FLOW PRESSURE READINGS

FIGURE 6: POWER SPECTRUM OF ZERO-FLOW BACKGROUND NOISE

IDLE ENGINE CONDITIONS

After the characterization of the background noise under zero-flow conditions, the Makila turboshaft gas turbine of the Bearcat test rig was started and kept at idle running conditions. As soon as the engine stabilized at idle conditions, 35

acquisitions of 5 seconds each were performed at a sampling frequency of 20 kHz. The statistical mean, standard deviation, skewness and kurtosis parameters of each measurement point were computed, and a dozen markedly erroneous measurement points have been observed, characterized by abnormally low mean pressure values, high standard deviation values, anormal skewness and kurtosis values or a combination thereof. After the 35th measurement point, the output signals V_P and V_S from the Kulite sensor became consistently erroneous, either flatlining, becoming extremely noisy or drastically increasing/decreasing beyond expected values. The tests were subsequently suspended, and the probe was visually inspected, showing signs of heavy soot contamination and significant condensation on the probe outer walls. Further tests proved impossible as the probe sensor appeared to be irremediably damaged.
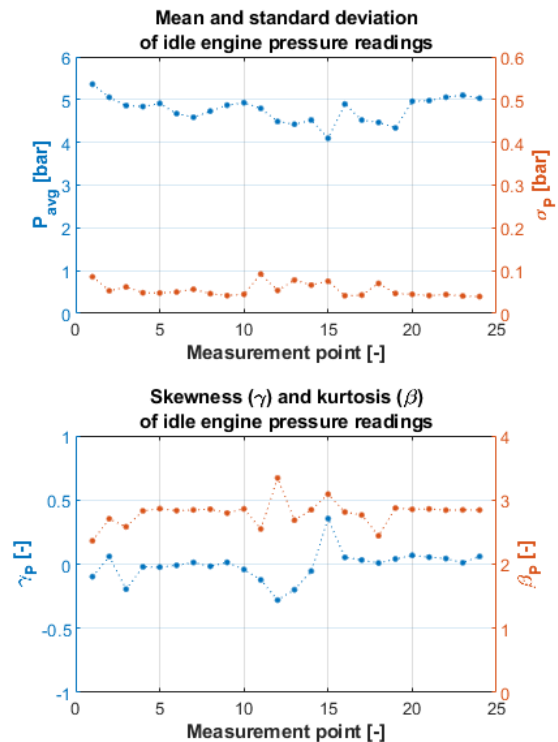

FIGURE 7: STATISTICAL MOMENTS OF THE 24 CURATED IDLE ENGINE PRESSURE READINGS

Despite the probe sensor failure, the acquired data, curated by removing 11 erroneous measurement points (FIGURE 7), were thoroughly processed and analysed. The mean pressure level measured in the measurement plane corresponding to the primary zone of the combustion chamber is $P_{avg} = [4.8 \pm 0.3]$ bar, roughly in line (albeit under-estimated by about 0.5 bar) with respect to pneumatic wall-static pressure measurements located in the high-pressure bypass annulus surrounding the combustor. The standard deviation

around the mean values is $\sigma_P = [0.06 \pm 0.02]$ bar, an order of magnitude higher than the zero-flow background noise pressure oscillations. The statistical moments skewness $\gamma_P = [-0.01 \pm 0.12]$ and kurtosis $\beta_P = [2.8 \pm 0.2]$ are in line with a normal Gaussian distribution around the mean value. Of main importance with regards to the effectiveness of the cooling, the temperature of the sensing element hovered around a mean value $T_{avg} = [80.1 \pm 3.5]$ °C (FIGURE 8), well below the target sensor surface temperature of 100 °C. An important comment is that the temperature did not fluctuate/increase uncontrollably before the sensor failure, which indicates that the probe cooling did not play a role in the chain of events that led to the critical sensor failure. This validates the effectiveness of the cooling layout around the fragile sensing element, which kept the sensor comfortably cool even at a relatively low (estimated) coolant flow rate around 0.5 – 1.5 l/min.
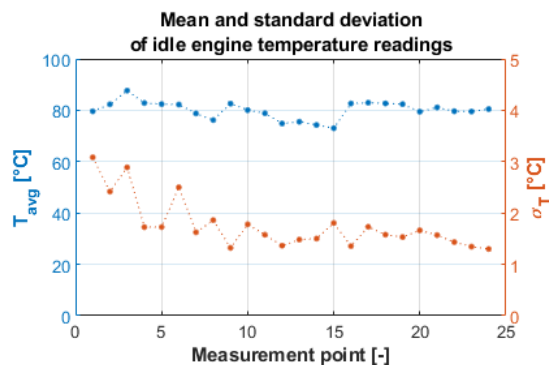
FIGURE 8: MEAN AND STANDARD DEVIATION OF THE 24 CURATED IDLE ENGINE TEMPERATURE READINGS

The power spectrum of the pressure readings, expressed in dB_{SPL} and averaged over the 24 curated measurement points, is shown in FIGURE 9. As a first observation, the measured sound pressure levels at idle engine conditions are on average 15 to 20 dB_{SPL} more powerful than the background noise measured at zero-flow conditions. Even though this qualifies as a quite low signal-to-noise ratio, the power spectrum at idle conditions is not overpowered by the background electronic noise of the sensor. Moreover, valuable and meaningful insights are obtained from the performed measurements. Multiple tonal peaks can clearly be observed across the frequency spectrum, with the bulk of the peaks identified as being harmonics to the fundamental of either the gas generator or the power turbine. The origin of the tonal peaks unrelated to the gas generator or the power turbine has not been clearly identified but could very well be linked to e.g. whistling flow through combustor dilution orifices or even excitation of the resonance frequency of various components of the combustion chamber, engine casing or the probe assembly. The

broadband noise on the other hand is characterized by a high-energy content in the low frequency region below 2 kHz, with a progressive decrease in sound pressure levels of 20 dB_{SPL} from 0.2 to 4 kHz, while beyond 4 kHz, the broadband noise remains relatively constant. However, an in-depth analysis of the combustion noise is well beyond the scope of the present paper and is in any case quite impossible using a single probe, as it typically requires multiple probes at various key locations for proper modal decomposition.
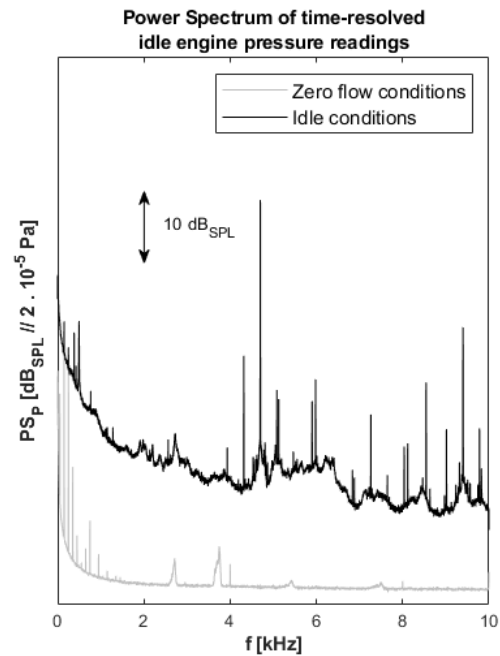

**FIGURE 9:** POWER SPECTRUM OF IDLE ENGINE PRESSURE READINGS

POST-TESTS REVIEW

After the curtailed experimental measurement campaign, the critically damaged prototype was destructively disassembled, allowing a thorough investigation of the root cause of the sensor failure by removing the protective screen in front of the sensing element. As can be clearly seen on FIGURE 11 (top left), soot penetrated the sensor cavity through the protective screen holes of the probe tip, and a layer of solidified soot particles fully covered the fragile sensing element of the Kulite. However, the sensing element itself did not appear to be irremediably destroyed, burnt nor damaged. Since soot is electrically conductive, it can be expected that the soot deposit shorts the Kulite circuit to ground and/or shorts parts of the piezo-resistor Wheatstone bridge, thereby leading to unsatisfactory excitation power to the sensor and/or erroneous output signals. After thoroughly removing the layer of soot from the sensor surface by means of a micro-brush and an ultrasonic bath (FIGURE 11 - top right), the behaviour of the sensing element fell back in line with the behaviour pre-failure (FIGURE 10 – blue dots), consequently

confirming that the soot deposit present on the Kulite chip was indeed the root cause of the critical sensor failure.

------- Pre-failure

⬤ Cleaned sensor
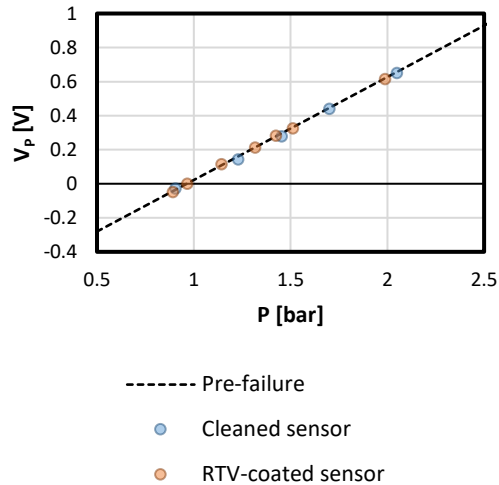
⬤ RTV-coated sensor

FIGURE 10: SENSOR SENSITIVITY AT AMBIENT TEMPERATURE (T = 20°C)
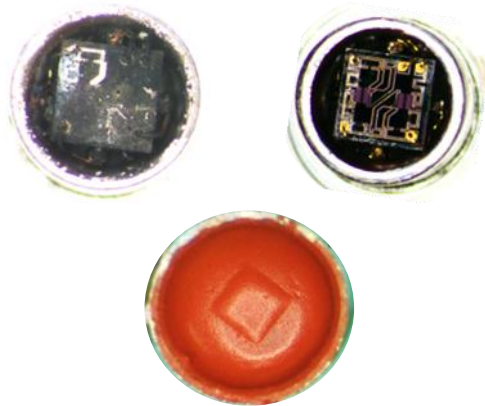
FIGURE 11: SOOT-CONTAMINATED SENSOR (TOP LEFT) – CLEANED SENSOR (TOP RIGHT) – RTV-COATED SENSOR (BOTTOM)

Since the presence of soot particles in the combustion chamber cannot be avoided, a solution is to further protect the fragile sensing element in addition to the use of a protective screened-recessed sensor layout. As recommended by Kulite [11], a layer of RTV coating has been applied on the restored sensing element (FIGURE 11 - bottom), shielding the fragile sensing element from external contaminants such as e.g. soot particles or even condensation droplets. Given that the recommended RTV-511 could not be obtained in time and in acceptable quantities, RTV-560 was identified as a fitting alternative. As was done after the cleaning of the soot-contaminated sensor, the sensitivity and dynamic response of the RTV-coated sensing element was compared to pre-failure behaviour, showing no impact of the RTV coating on neither the sensitivity (FIGURE 10 – red dots) nor the dynamic response.

At the time of writing this paper, no additional tests on the Bearcat test rig have been performed with a newly assembled probe equipped with the RTV-coated sensor. As such, the proposed solution described here above could not yet be verified through engine-representative tests.

CONCLUSIONS

In this paper, a short summary of the methodology used for the design of a water-cooled fast-response wall-static pressure probe intended for measurements in the combustion chamber of gas turbines is presented. In addition, the results from a series of tests performed with the first prototype of the probe mounted in the primary zone of the combustion chamber of a turboshaft gas turbine test rig are discussed.

Background noise measurements under zero-flow conditions have indicated that the prototype's XCE-062 250 PSIA sensor behaves as a microphone with a quite high noise floor. However, acoustic noise in the combustor is expected to be well above the aforementioned noise floor.

The measurements performed with the Bearcat test rig running at idle engine conditions had to be curtailed as the prototype's sensor critically failed after 32 minutes of effective testing time and 4 engine starts. However, the measured and curated data delivered valuable insights, especially with regards to the power spectrum characterized by multiple tonal peaks which could be clearly identified. The signal-to-noise ratio derived from the power spectrum lies quite satisfactorily between 15 and 20 dB_{SPL}. Moreover, the sensor cooling layout behaved as intended, with a sensor surface temperature not exceeding 80 °C during the tests.

The destructive disassembly of the critically damaged prototype allowed to identify heavy soot contamination of the screened-recessed cavity as the reason for the sensor failure. A thorough cleaning of the sensor allowed to restore the signal, and a sensor re-packaging was proposed using RTV-560 as a protective coating, which does not interfere with the sensitivity nor the dynamic response of the sensor.

ACKNOWLEDGEMENTS

REFERENCES

[1]   Kurtz, A. D., and Ned, A. A., 2004. "Ultra-High Temperature Miniature SOI Sensors for Extreme Environments". In Proceedings of IMAPS International HITEC Conference.

[2]   Ned, A.A., Kurtz, A.D., Beheim, G., Masheeb, F. and Stefanescu, S., 2004. "Improved Sic Leadless Pressure Sensors for High Temperature, Low and High Pressure Applications". In Twenty-First Transducer Workshop.

[3]   Ferguson, D. G. and Ivey, P. C., 1998. "A High-Temperature Assessment of Air-Cooled Unsteady Pressure Transducers". Transactions of the ASME, 120, June, pp. 608-612.

[4]   Ivey, P. C. and Ferguson, D. G., 2002. "An Air-Cooled Jacket Designed to Protect Unsteady Pressure Transducers at Elevated Temperatures in Gas Turbine Engines". In Proceedings of ASME Turbo Expo 2002. June 3 – 6, 2002, Amsterdam, The Netherlands.

[5]   Brouckaert, J.-F., Mersinligil, M. and Pau, M., 2008. "A Conceptual Design Study for a New High Temperature Fast Response Cooled Total Pressure Probe". In Proceedings of ASME Turbo Expo 2008. June 9 – 13, 2008, Berlin, Germany.

[6]   Mersinligil, M., Brouckaert, J.-F. and Desset, J., 2010. "First Unsteady Pressure Measurements with a Fast Response Cooled Total Pressure Probe in High Temperature Gas Turbine Environments". In Proceedings of ASME Turbo Expo 2010. June 14 – 18, 2010, Glasgow, United Kingdom.

[7]   Doebelin, E. O., 1990. "Measurement Systems Application and Design". Fourth Ed., McGraw-Hill Publishing Co., pp. 473 – 482.

[8]   Hougen, J. O., Martin O. R. and Walsh, R. A., 1963. "Dynamics of Pneumatic Transmission Lines", Control Eng., 10:114-117.

[9]   Clinckemaillie, J. and Fontaneto, F. "Cooled Pressure Probes Design Methodology for Harsh Environment Applications". In Proceedings of ASME Turbo Expo 2020. June 22-26, 2020, London, United Kingdom.

[10]   Champion-Réaud, J.-L., Bidan, G., Breining, J.-L., Lambert, P.-A., Mendes, C. and Zouloumian, N. "BEARCAT: The SAFRAN Brand New Test Engine Heavily Instrumented for Accurate Comparison With CFD Calculations". In Proceedings of ASME Turbo Expo 2020. June 22-26, 2020, London, United Kingdom.

[11]   Hurst A. M., Olsen T. R., Goodman S., VanDeWeert J. and Shang T. "An Experimental Frequency Response Characterization of MEMS Piezoresistive Pressure Transducers". In Proceedings of ASME Turbo Expo 2014. June 16 – 20, 2014, Düsseldorf, Germany.